J. Synchrotron Rad. (1998). **5**, 1020–1022

Improvement of spectrometer energy resolution for high-resolution photoelectron spectroscopy

H. Iwai,[a]* H. Namba,[a] Y. Kido,[a] M. Taguchi[b] and R. Oiwa[b]

[a]*Department of Physics, Faculty of Science and Engineering, Ritsumeikan University, Kusatsu-shi 525, Japan, and* [b]*ULVAC-PHI Inc., Chigasaki 253, Japan.*
E-mail: iwai@ff.iij4u.or.jp

(*Received 4 August 1997; accepted 11 December 1997*)

For high-energy-resolution photoelectron spectroscopy using synchrotron radiation, the energy resolution of a commercial compact photoelectron spectrometer (hemispherical concentric spectrometer) was improved by reducing the size of the entrance and detector slits and optimizing the operation conditions of the lens voltage. Under the optimized conditions, ray-tracing simulations show that severe spectral intensity decreases can be avoided. An energy resolution of 6.2 meV and a resolving power of 8100 at a kinetic energy of 50 eV were experimentally obtained.

Keywords: concentric hemispherical analysers; energy resolution; photoelectron spectroscopy; ray-tracing simulation; resolving power.

1. Introduction

X-ray photoelectron spectroscopy (XPS) is a useful method for simultaneous analysis of chemical and bonding states on surfaces. High-energy-resolution XPS and vacuum ultraviolet photoelectron spectroscopy (UPS) are now available using an incident light source of narrow energy width obtained from synchrotron radiation. In such cases, a concentric hemispherical analyser (CHA) is commonly used as an electron spectrometer as it is suitable for energy analysis in high-energy-resolution photoelectron spectroscopy and angle-dependent photoelectron spectroscopy (Osterwalder *et al.*, 1989; Mårtensson *et al.*, 1994). The CHA (PHI 10-360) has been used at the high-resolution vacuum ultraviolet (VUV) beamline SORIS (Kido *et al.*, 1998; Namba *et al.*, 1998) at Ritsumeikan University to measure XPS and UPS in the study of surface electronic states, such as the one-dimensional nature of the step on stepped surfaces (Namba, 1996). In such cases, it is necessary to acquire a high-resolution core-level photoelectron spectrum and a fine-structure spectrum of the valence band. However, the CHA, which was manufactured as a high-transmission analyser for small-area analysis, has an energy resolution of about 40 meV, which is insufficient for the requirements of our study.

It is known that high energy resolution can be obtained by reducing the analyser slit size or the pass energy. For a compact CHA which has hemispheres of a small mean radius, the reduction in transmission should be considered when reducing the slit size, as the analysis area and the acceptance angle may be reduced. The dependence of transmission on the slit size, lens magnification, pass energy and kinetic energy is quite complicated. Therefore optimization of the slit size and the pass energy by ray-tracing simulation and experiment is very important in minimizing the decrease in transmission.

In this paper, we discuss the optimization and modification of the compact CHA in order to improve the energy resolution with the aim of achieving an energy resolution of less than 10 meV. Some evaluation results are also reported.

2. Analyser modification for improvement of energy resolution

The energy resolution ΔE, defined as full width at half-maximum (FWHM), for a CHA is given by

$$\Delta E = [(w/2R) + (\alpha^2/4)]E_p, \quad (1)$$

where E_p is the pass energy of the analyser, w is the slit width of the analyser, R is the mean radius of the hemispheres and α is the half-angle of electrons entering the analyser at the entrance slit (Briggs & Seah, 1990). Relative resolution is sometimes also expressed as the resolving power ρ in terms of the initial kinetic energy E_0 and ΔE, *i.e.*

$$\rho = E_0/\Delta E. \quad (2)$$

High energy resolution may be achieved by decreasing the pass energy; however, this may not give good analyser transmission and energy resolution. One reason is that the transmission of the analyser input lens is also decreased by a higher retarding ratio, which is defined as initial kinetic energy divided by pass energy (Seah & Smith, 1990). Another reason is that contamination on the electrode surfaces may cause distortion of the electric field in both hemispheres, restricting the transmission and energy resolution. Thus, we consider changing the slit width w and the half-angle α as estimated by the ray-tracing simulation.

Fig. 1 shows a diagram of the analyser and related electronics (Physical Electronics, 1986). The analyser, as originally designed

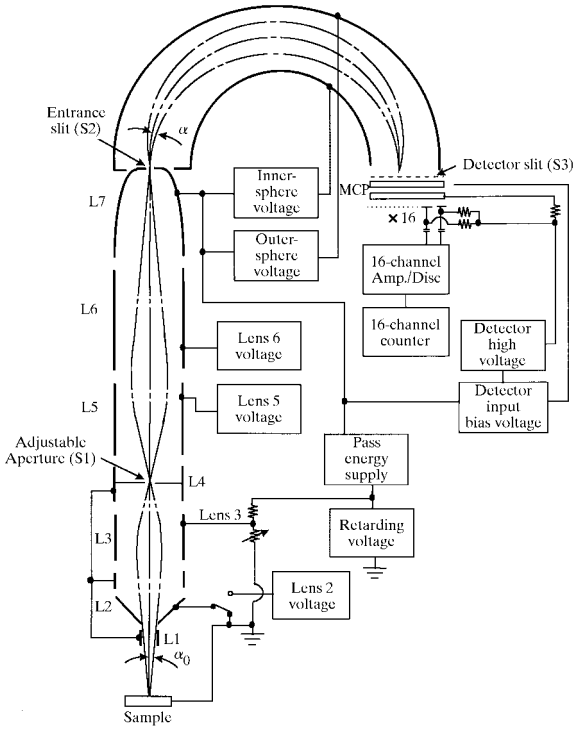

Figure 1
Diagram of the concentric hemispherical analyser and related electronics.

Table 1
Experimental results of the energy resolution and resolving power at 50 eV kinetic energy.

Pass energy (eV)	Measured peak width (meV)	Theoretical peak width (meV)	Energy resolution (meV)	Resolving power
0.585	7.3	4.1	6.2	8100
1.175	8.2	4.6	7.2	6900
2.950	9.8	7.3	9.0	5600
5.850	13.3	12.8	12.7	3900
11.750	25.1	24.9	24.8	2000
23.500	49.4	49.4	49.2	1000

by Physical Electronics, is configured with an analyser input lens, spheres and 16-channel detector using a chevron-mounted pair of microchannel plates. The input lens is a double-focused lens with seven lens elements. The first stage (L1–L4) of the input lens defines the analysis area selected by the adjustable aperture S1. The magnification and acceptance angle are changed by adjusting the L2 and L4 voltages. The second stage (L5–L7) of the input lens functions as a transfer lens to the CHA. The sizes of the entrance slit S2 and the detector slit S3 are 4 × 10 mm and 2 × 19 mm, respectively. The half-angle of electrons entering the analyser, α, was estimated as 2° at an L2 operating voltage of 0 V by ray-tracing simulation. Therefore, the expected energy resolution was calculated to be 14 meV at 1 eV pass energy.

To improve the energy resolution, the sizes of S2 and S3 were changed to 0.4 × 10 mm and 0.5 × 19 mm, respectively. The surfaces of the lens elements, spheres and detector were coated with graphite rather than gold to reduce secondary electron scattering. The energy resolution at a pass energy of 1 eV was then calculated to be 2.1 meV.

3. Experimental apparatus

To evaluate the energy resolution of the analyser, spectra of the transmitted electron beam were measured. The half-solid-angle for the monochromated electron beam is about 2° with a 20 mm working distance which is adjustable by varying the external voltage supply. The working distance of the input lens for the analyser is about 19 mm. The monochromator, composed of an electron gun, an energy analyser and a lens, was shielded with two separate continuous layers of μ-metal. The monochromatic electron beam can be moved mechanically in the x, y and z directions from outside the vacuum chamber. The mean radius of the monochromator hemispheres is 50 mm and the entrance slit size is 0.2 × 5 mm. The half angle α was estimated to be 3.2° at 1.4 eV pass energy from the ray-tracing simulation of the input lens. Therefore, the energy resolution was calculated to be 3.9 meV FWHM at 1.4 eV pass energy, which was sufficient for the present experiment.

The voltage range of the retarding power supply for the analyser was modified from 0–320 V with 5 mV step to 0–64 V with 1 mV step for high-energy-resolution measurement. The ripple voltage was less than 2 mV at 50 V. In addition, the commercial software was modified for the new voltage range.

The beam voltage, filament current and pass energy of the electron gun were set to 50.000 V, 2.45 A and 1.400 eV, respectively. The beam current obtained from the monochromator was about 0.1 pA. The spectra were recorded in channel 8 of a 16-channel detector using a 0.125 mm-diameter adjustable aperture S1 with a 1 meV energy step and a recording time of 0.655 s step^{-1} with 10 sweeps. The pressure was maintained at about 1 × 10^{-7} Pa during the measurement.

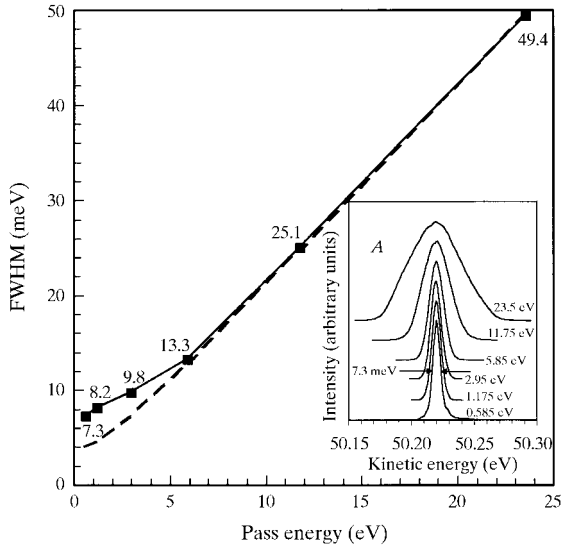

Figure 2
Experimentally obtained FWHM (solid line) and theoretically calculated FWHM (dashed line) of the transmitted electron-beam spectra as a function of the pass energy. Labels show the values of experimentally obtained FWHM. Inset *A* shows the transmitted electron-beam spectra.

4. Results and discussion

The peak width and the peak profile of the transmitted electron beam recorded as a function of pass energy are shown in Fig. 2. The energy resolution and the resolving power are summarized in Table 1. The spectrum at 0.585 eV pass energy was measured with a 0.5 mm-diameter adjustable aperture S1, as the count rate was extremely low (about 70 counts s^{-1}). The minimum peak width of the transmitted electron-beam spectra at 50 eV kinetic energy was 7.3 meV at 0.585 eV pass energy (and a retarding ratio of 85). The energy resolution and resolving power of the analyser were calculated as 6.2 meV and 8100, respectively, assuming the energy width of the monochromated electron beam to be 3.9 meV. These values are sufficient for our study. The experimentally obtained FWHM curve is in good agreement with the theoretically calculated FWHM curve above 5.85 eV pass energy. Below 5.85 eV pass energy, the experimentally obtained peak width was slightly greater than the theoretically calculated peak width. One reason is that the imperfection of the alignment and optimization of the lens voltage for the CHA may defocus the transmitted electron beam at the detector slit. Slight contamination of the hemispheres of the CHA may also cause electric field distortion due to changes in the work function of the hemispheres. Additionally, the energy width of the monochromated electron beam assumed in the calculation may not be correct for similar reasons, such as contamination of the monochromating analyser of the electron gun or misalignment of the electron-gun lenses.

From the ray-tracing simulation, the magnification of the lens was found to be 1.5, which can be ignored with a 0.125 mm-diameter adjustable aperture S1. The reduction rate of transmission for the modified analyser is estimated to be about 25% of that of the original analyser at the same pass energy, corresponding to the decrease in transmission from changing the size of the detector slit. On the other hand, the original analyser must be operated at 17% lower pass energy than that of the modified analyser to achieve the same energy resolution. The reduction rate of transmission for the original analyser was evaluated as 11% at these retarding ratios (Tanaka, 1995), therefore the change in transmission for the modified analyser can be estimated as 1.5 times higher than that of the original analyser.

5. Conclusions

The energy resolution and the resolving power of the commercial compact CHA at 50 eV kinetic energy were improved to 6.2 meV and 8100, respectively. Reconsidering the design and operation of the analyser at a high retarding ratio can improve the energy resolution considerably without any decrease in the transmission rate by optimization of the slit size and lens voltages using a ray-tracing simulation.

References

Briggs, D. & Seah, M. P. (1990). Editors. *Practical Surface Analysis*, 2nd ed., Vol. 1, pp. 70–80. Chichester: John Wiley.

Kido, Y., Namba, H., Nishimura, T., Ikeda, A., Yan, Y. & Yagishita, A. (1998). *Nucl. Instrum. Methods B*. In the press.

Mårtensson, N., Baltzer, P., Brühwiler, P. A., Forsell, J.-O., Nilsson, A., Stenborg, A. & Wannberg, B. (1994). *J. Electron Spectrosc. Relat. Phenom.* **70**, 117–128.

Namba, H. (1996). *Surf. Sci.* **357/358**, 238–244.

Namba, H., Obara, M., Kawakami, D., Nishimura, T., Yan, Y., Yagashita, A. & Kido, Y. (1998). *J. Synchrotron Rad.* **5**, 557–558.

Osterwalder, J., Sagurton, M., Orders, P. J., Fadley, C. S., Hermsmeier, B. D. & Friedman, D. J. (1989). *J. Electron Spectrosc. Relat. Phenom.* **48**, 55–99.

Physical Electronics (1986). Technical Bulletin No. 8601. Physical Electronics Inc., 6509 Flying Cloud Drive, Eden Prairie, Minnesota 55344, USA.

Seah, M. P. & Smith, G. C. (1990). *Surf. Interface Anal.* **15**, 751–766.

Tanaka, A. (1995). *J. Surf. Anal.* **1**, 189–209.